Article

SOURCE DATA TRANSPARENT PROCESS OPEN ACCESS

EMBO reports

Transcription factor p63 bookmarks and regulates dynamic enhancers during epidermal differentiation

Evelyn N Kouwenhoven[1,2], Martin Oti[2], Hanna Niehues[3], Simon J van Heeringen[2], Joost Schalkwijk[3], Hendrik G Stunnenberg[4], Hans van Bokhoven[1] & Huiqing Zhou[1,2,*]

Abstract

The transcription factor p63 plays a pivotal role in keratinocyte proliferation and differentiation in the epidermis. However, how p63 regulates epidermal genes during differentiation is not yet clear. Using epigenome profiling of differentiating human primary epidermal keratinocytes, we characterized a catalog of dynamically regulated genes and p63-bound regulatory elements that are relevant for epithelial development and related diseases. p63-bound regulatory elements occur as single or clustered enhancers, and remarkably, only a subset is active as defined by the co-presence of the active enhancer mark histone modification H3K27ac in epidermal keratinocytes. We show that the dynamics of gene expression correlates with the activity of p63-bound enhancers rather than with p63 binding itself. The activity of p63-bound enhancers is likely determined by other transcription factors that cooperate with p63. Our data show that inactive p63-bound enhancers in epidermal keratinocytes may be active during the development of other epithelial-related structures such as limbs and suggest that p63 bookmarks genomic loci during the commitment of the epithelial lineage and regulates genes through temporal- and spatial-specific active enhancers.

Keywords epidermal differentiation; epigenomics; gene regulation; p63
Subject Categories Development & Differentiation; Stem Cells; Transcription
DOI 10.15252/embr.201439941 | Received 2 December 2014 | Revised 11 March 2015 | Accepted 20 April 2015 | Published online 1 June 2015
EMBO Reports (2015) 16: 863–878

Introduction

Orchestrated spatial and temporal gene regulation during embryonic development is essential for proper organogenesis. The transcription factor p63 is a key regulator in epithelial development including the development of epidermis, limbs, and craniofacial tissues. The role of p63 in epithelial lineage commitment has been demonstrated by many studies in human diseases and mouse models. In humans, heterozygous mutations in the *TP63* gene are associated with at least seven clinical conditions where epithelial-related structures are affected, characterized by combinations of ectrodactyly (split hand/foot malformations), orofacial clefting, and ectodermal dysplasia [1]. Several *p63* mouse models including knockouts and knock-ins with *TP63* disease mutations show similar developmental and structural defects as those in human p63-associated diseases [2–6]. In mouse embryonic stem cells, knockdown of *p63* or overexpression of *p63* mutants associated with diseases prevented the epithelial commitment marked by *KRT5/KRT14* expression [7,8].

The epidermis is one of the affected epithelial structures in *p63*-associated disorders and in *p63* mouse models. The human epidermis is a multilayered epithelial tissue, and the structural integrity of the epidermis is dependent on proper proliferation and differentiation of epidermal keratinocytes. The epidermal basal layer consists of highly proliferative self-renewing keratinocytes. Upon initiation of differentiation, keratinocytes migrate upwards and differentiate into cells that comprise the suprabasal spinous layer, the granular layer, and the stratum corneum that consists mainly of enucleated corneocytes [9]. The differentiation process of keratinocytes is tightly controlled by gene regulation, and de-regulated gene expression leads to disturbed epidermal differentiation and skin diseases [10]. Many epidermal disease genes are expressed in specific layers of the epidermis and associated with distinct disease phenotypes. In general, mutations in genes that are highly expressed in the basal layers such as keratin 5 (*KRT5*) and keratin 14 (*KRT14*) are associated with blistering phenotypes [11], whereas mutations in genes that are expressed in the most outer layers of the epidermis, such as loricrin (*LOR*), are associated with hyperkeratosis and dry or scaly skin [10,12]. Although significant progress has been made in genetic studies with the fast-developing next-generation sequencing technology, the causes of many skin diseases are not yet explained. Furthermore, many of these conditions are heterogeneous, suggesting that the expressivity of gene mutations is modulated by genetic

1 Department of Human Genetics, Radboud Institute for Molecular Life Sciences, Radboud University Medical Center, Nijmegen, The Netherlands
2 Department of Molecular Developmental Biology, Faculty of Science, Radboud Institute for Molecular Life Sciences, Radboud University, Nijmegen, The Netherlands
3 Department of Dermatology, Radboud Institute for Molecular Life Sciences, Radboud University Medical Center, Nijmegen, The Netherlands
4 Department of Molecular Biology, Faculty of Science, Radboud Institute for Molecular Life Sciences, Radboud University, Nijmegen, The Netherlands
*Corresponding author. Tel: +31 24 3616851; E-mail: jo.zhou@radboudumc.nl; j.zhou@science.ru.nl

© 2015 The Authors. Published under the terms of the CC BY NC ND 4.0 license

modifiers that play roles in epidermal differentiation. This scenario is supported by the observation that epidermal differentiation is regulated by the interplay of diverse gene networks rather than individual genes [13]. Therefore, comprehensive catalogs of gene networks that are controlled by key regulators such as the transcription factor p63 during epidermal differentiation will be instructive for understanding the molecular processes underlying skin disease.

It has been shown that *p63* is essential for the initiation of epidermal differentiation. In human epidermal keratinocytes, knockdown of *p63* prevents epidermal differentiation [14], whereas in single-layered lung epithelial cells, overexpression of *p63* results in stratification that is normally typical for epidermal keratinocytes [15]. Human epidermal keratinocytes established from patients with *TP63* mutations show stratification defects [16]. A number of studies have aimed at the identification of p63 target genes to understand the role of p63 in epidermal differentiation. Some studies took the RNAi approach to knock down *p63* in proliferating keratinocytes and identified several hundreds of potentially p63-regulated genes [14,17]. However, as *p63*-depleted keratinocytes have differentiation defects [14,17], potential direct p63 target genes at later stages of epidermal differentiation might not be identified using this approach. Furthermore, ChIP-seq analysis in human epidermal keratinocytes identified tens of thousands p63 binding sites in the human genome [18,19]. The large difference between the number of p63 binding sites [18,19] and p63-regulated genes found using RNAi approaches [14,17] raises the question whether all identified p63 binding sites are functional in gene regulation in epidermal keratinocytes. Here, we present the first comprehensive catalog of p63-regulated genes and enhancers during epidermal differentiation through epigenomics and transcriptomics profiling. Only a subset of these enhancers is dynamically regulated, and the activity of these enhancers marked by the active enhancer histone modification H3K27ac correlates with gene expression during epidermal differentiation.

Results

Gene expression dynamics during epidermal differentiation

Using an *in vitro* differentiation model of human epidermal keratinocytes [16,20], we generated a complete map of dynamically regulated genes during epidermal differentiation at a genomewide scale using RNA polymerase II (RNAPII) ChIP-seq that measures the occupancy of RNAPII in mainly gene-associated genomic regions, as well as RNA-seq that measures the steady-state mRNA level. With both methods, the detected expression pattern of epidermal marker genes such as *KRT5*, *KRT1,* and *involucrin* (*IVL*) (Fig 1A), and *KRT14, KRT10* and *loricrin* (*LOR*) (Supplementary Fig S1A) was consistent with our RT–qPCR and Western blotting analyses (Supplementary Fig S1B and C). Expression of these marker genes was also in agreement with their expression dynamics *in vivo* [20,21]. At the global level, our RNA-seq analysis showed a good correlation (Spearman rho > 0.8 for all comparisons) with a previous RNA-seq study that used a slightly different *in vitro* keratinocyte differentiation method (Supplementary Fig S2A) [22]. Thus, our results show that this *in vitro* differentiation model of epidermal keratinocytes recapitulates the epidermal stratification process. Of note, RNAPII ChIP-seq and RNA-seq profiles at the *TP63* locus showed that Δ*Np63* is the main isoform expressed in keratinocytes throughout the epidermal differentiation process, and the expression of the *TAp63* isoform was not detected with both RNAPII ChIP-seq and RNA-seq methods (Supplementary Fig S1D). Western blot analysis confirmed the decreased protein level of ΔNp63 during differentiation and that the expression of TAp63 was undetectable (Supplementary Fig S1B). The decreased Δ*Np63* expression at the mRNA and protein levels is in agreement with previous reports [16,23].

To capture the gene expression dynamics during differentiation, we clustered the genes according to their expression levels quantified as reads per kilobase per million mapped reads (RPKM) in both the RNAPII ChIP-seq and RNA-seq profiles. For RNAPII ChIP-seq analyses, 7,223 genes with an RPKM value (expression level) of at least 1.0 were clustered using K-means clustering into nine groups with distinct expression patterns (Fig 1B; Supplementary Table S1A). To assess the function of these gene clusters and their association with human diseases, we performed functional annotation analyses using the web tools DAVID Gene Ontology (GO) [24] (Fig 1B; Supplementary Table S1B) and the Human Phenotype Ontology (HPO) database [25] (Supplementary Table S1C), respectively. For examples, genes that are expressed highly in proliferating keratinocytes (cluster 4) are associated with skin blistering and hyperkeratosis (e.g., *KRT5*). Genes that are highly expressed at late differentiation stages (cluster 3, e.g., *LCE* genes and cluster 6, e.g., *TGM1*) are specifically enriched for late differentiation genes and those involved in the regulation of apoptosis and cell death. These genes are associated with dry and scaly skin and non-blistering phenotypes. Cluster 1 contains genes with high expression at early differentiation stages (day 2 and day 4) and reduced expression at the late stage (day 7), for example *KRT1* and *KRT10*, and is enriched with genes involved in epidermis development, blistering, and hyperkeratosis. For the RNA-seq analyses, we identified 3,813 genes that were significantly differentially expressed between keratinocyte differentiation stages (P-value < 0.05, cuffdiff2 software) and with an RPKM > 10 in at least one stage. Six distinct gene clusters were defined based on the expression dynamics of these genes using K-means clustering (Supplementary Fig S2B; Supplementary Table S2A). Similar to the RNAPII ChIP-seq data, the RNA-seq data also showed that genes with distinct expression patterns during epidermal differentiation are associated with distinct roles during epidermal differentiation and with different skin disease phenotypes (Supplementary Fig S2B; Supplementary Table S2B and C).

We further investigated and compared gene expression detected by RNAPII ChIP-seq and by RNA-seq. The global analysis showed that the range of expression levels (RPKM values) is narrower in the RNAPII ChIP-seq profile than in the RNA-seq profiles (Supplementary Fig S2C). Nevertheless, the relative expression levels of genes (gene ranks based on their RPKM) are generally similar in both RNAPII ChIP-seq and RNA-seq profiles (Supplementary Fig S2D, Supplementary Table S3A), as the relationship between RNAPII occupancy and steady-state mRNA level remains largely unchanged during epithelial differentiation for most genes. However, a small proportion of genes showed substantially higher RNAPII occupancy than mRNA levels (Supplementary Fig S2D, the bottom cluster), and these genes are strongly enriched for non-coding RNAs (mean-rank gene set enrichment, P-value < 10^{-95} at all stages) (Supplementary Table S3C and D). Despite the global similarity, closer inspection

 © 2015 The Authors

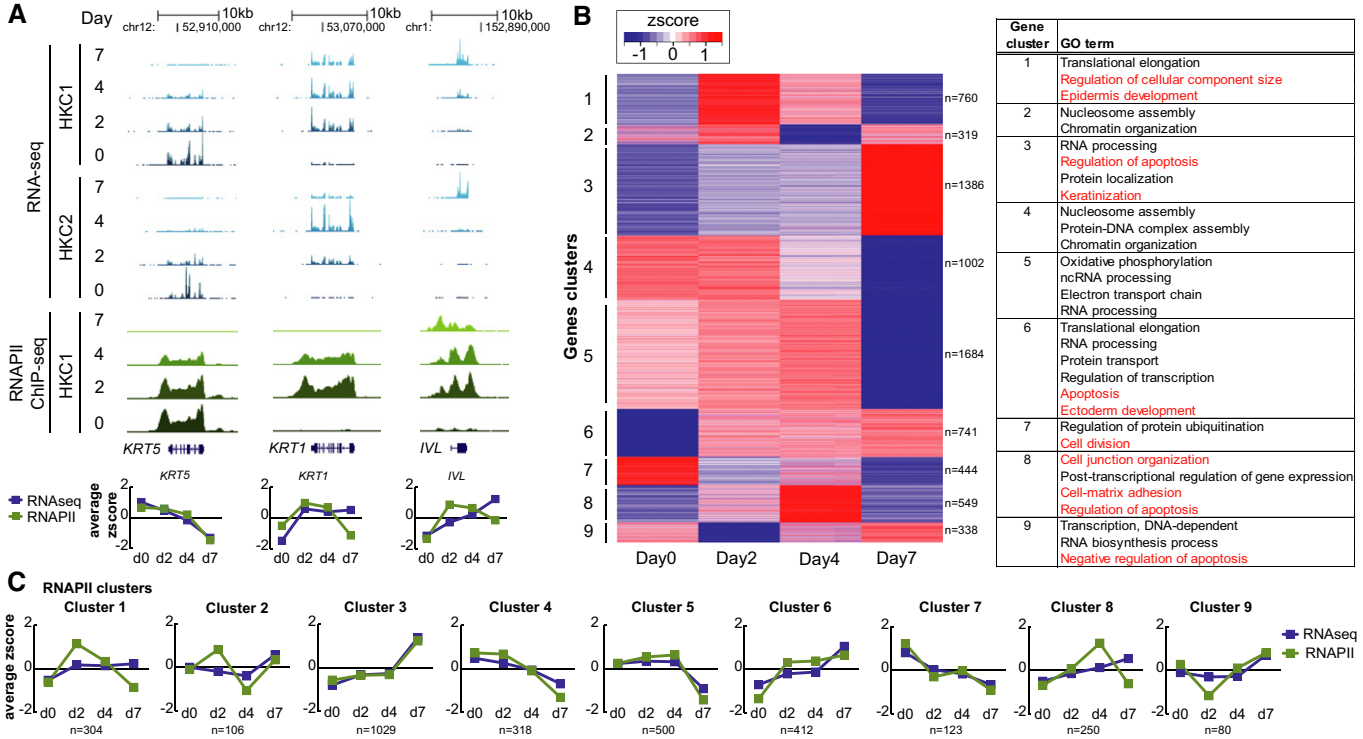

Gene cluster	GO term
1	Translational elongation Regulation of cellular component size Epidermis development
2	Nucleosome assembly Chromatin organization
3	RNA processing Regulation of apoptosis Protein localization Keratinization
4	Nucleosome assembly Protein-DNA complex assembly Chromatin organization
5	Oxidative phosphorylation ncRNA processing Electron transport chain RNA processing
6	Translational elongation RNA processing Protein transport Regulation of transcription Apoptosis Ectoderm development
7	Regulation of protein ubiquitination Cell division
8	Cell junction organization Post-transcriptional regulation of gene expression Cell-matrix adhesion Regulation of apoptosis
9	Transcription, DNA-dependent RNA biosynthesis process Negative regulation of apoptosis

Figure 1. Transcriptional and expression dynamics of epidermal differentiation.

A Screenshot of the UCSC genome browser from normalized RNA-seq and RNAPII ChIP-seq data during keratinocyte differentiation (days 0, 2, 4 and 7 after differentiation initiation) at gene loci of differentiation markers (*KRT5*, *KRT1*, and *IVL*). RNAPII ChIP-seq dataset was generated from human primary keratinocytes of one donor (HKC1). RNA-seq datasets were generated from human primary keratinocytes of two donors (HKC1 and HKC2). Expression dynamics of RNA-seq (in blue) and RNAPII ChIP-seq (in green) represented by the average *z*-scores (calculated from $\log_2$ (RPKM)) were plotted for *KRT5*, *KRT1*, and *IVL* for all keratinocyte differentiation stage (days 0, 2, 4, and 7) of HKC1.

B Heatmap of RNAPII expression patterns of differentially transcribed genes at days 0, 2, 4, and 7 during differentiation by K-means clustering analysis. Genes with an *RPKM* > 1 at any differentiation stage are included (*n* = number of genes per cluster). Enriched GO terms of genes per gene cluster are summarized in the table on the right (complete data summarized in Supplementary Table S1A).

C Expression dynamics of RNA-seq (in blue) and RNAPII ChIP-seq (in green) represented by the average *z*-scores (calculated from $\log_2$ (RPKM)) were plotted from genes in each RNAPII gene cluster for all differentiation stages (days 0, 2, 4, and 7). Standard deviations for genes per stage in each cluster are summarized in Supplementary Table S20.

reveals different dynamics of gene expression patterns between these two methods for many genes (Fig 1A and C). For example, the highest expression level of *KRT10* was detected at differentiation day 2 in RNAPII ChIP-seq, while its expression in the RNA-seq profile only reached its highest level at day 4 (Supplementary Fig S1A). The expression pattern detected in the RNA-seq analysis correlates with the protein levels (Supplementary Fig S1B). Consistent with the expression of individual marker genes, expression patterns of genes in the RNAPII ChIP-seq clusters were often more dynamic than their corresponding RNA-seq expression patterns, with the expression changes in the RNAPII ChIP-seq profiles preceding those in the RNA-seq profiles (Fig 1C). These observations are consistent with RNAPII-mediated transcription preceding mRNA buildup and highlight differences between transcription rate control and steady-state mRNA level maintenance. Interestingly, Spearman correlation analysis showed a slightly better correlation of H3K27ac levels with the RNAPII occupancy at gene bodies than with the steady-state mRNA abundance (Supplementary Fig S2E). This may reflect the influence of post-transcriptional processes such as RNA stability and processing of mRNA by miRNAs on mRNA steady-state levels. These data suggest that RNAPII ChIP-seq is a preferred method to study the direct effect of transcription factors on gene regulation as compared to RNA-seq. Based on this rationale, we used the RNAPII occupancy at the gene body as the measure of gene expression to study the p63-regulated transcription in subsequent analyses.

MicroRNAs (miRNAs) have been shown to play an important role in epidermal differentiation [26–28], and therefore we analyzed our RNA-seq and RNAPII ChIP-seq for expression of miRNAs. Examining the RNAPII occupancy at annotated miRNA genes using K-means clustering analysis showed dynamically regulated expression of 103 primary miRNA (pri-miRNA) transcripts during differentiation (Supplementary Fig S3A; Supplementary Table S4A) [29]. Some of these miRNAs have been reported to play a role in epidermal differentiation such as *miR-205* and *miRNA-203* (Supplementary Fig S3B) [27,30,31]. For most of these miRNAs, RNA-seq signals at miRNA regions are low and the correlation between RNAPII ChIP-seq and RNA-seq signals is poor (Supplementary Table S4C). Thus, RNAPII occupancy appears to give a better readout of pri-miRNA transcription.

© 2015 The Authors

p63-bound enhancers during epidermal differentiation

Next, we assessed the role of p63 in regulating dynamic gene expression during epidermal differentiation. We performed ChIP-seq of p63 from keratinocytes at different stages of differentiation. Among a total number of 38,980 p63 binding sites detected from all stages (Supplementary Table S5E), more than 90% were found to contain at least one p63 binding consensus motif using our previously established p63scan algorithm [18], and there is a significant enrichment of p63 binding in promoter regions and within 25 kb distance of genes compared to genomic distributions of all binding sites (hypergeometric test, *P*-value < 1E-323 and *P*-value = 6.97E-174, respectively) (Supplementary Fig S4A). Surprisingly, in contrast to the dynamic gene expression pattern observed in RNAPII ChIP-seq and RNA-seq analyses (Fig 1C), the number of p63 binding sites and the p63 binding signals only showed a minor overall decrease during differentiation (Fig 2A; Supplementary Fig S4B). This is probably due to the decreasing p63 protein levels during epidermal differentiation (Supplementary Fig S1B) [16,23].

To resolve the seeming inconsistency between the rather static p63 binding and the dynamic gene expression during differentiation, we examined the epigenetic state of p63 binding sites using ENCODE data of primary human keratinocytes (NHEK) [32]. Of all p63 binding sites, 50.5% are co-localized with the H3K27ac histone mark associated with active enhancers (Supplementary Table S6A). This suggests that approximately half of the identified p63-bound regions are active enhancer elements in human keratinocytes. H3K27me3 and H3K9me3, repressive histone modification marks associated with poised enhancers in embryonic stem cells and heterochromatin [32,33], respectively, were not detected at any of the identified p63 binding sites (Fig 2A), even though these marks are present at promoters of inactive genes (examples in Supplementary Fig S5A). As ENCODE data of NHEKs were collected at only one condition and provide limited information for the transcription program during epidermal differentiation, we further investigated the H3K27ac occupancy at all four stages during epidermal differentiation to gain insight into the activity dynamics of the p63-bound regions. Our data showed that 56.9% of all identified p63 binding sites were co-occupied by H3K27ac at any of the four stages (Supplementary Table S6B–F), consistent with the ENCODE data analysis (Fig 2A; Supplementary Table S6A). The p63 binding sites with a detectable level of H3K27ac were considered as active p63 binding sites. When active p63 binding sites were mapped to adjacent genes (Supplementary Table S6G), a strong correlation was observed between the RNAPII occupancy at most genes and H3K27ac levels at the nearby p63 binding sites across the four stages of differentiation (median Pearson's R = 0.77) (Fig 2B). In contrast, the p63 levels at these binding sites showed no tendency to correlate with nearby gene body RNAPII levels during differentiation (median Pearson's R = 0.09). These results indicate that H3K27ac occupancy at p63 binding sites, rather than p63 occupancy itself, reflects the regulatory activity of p63 binding sites in the transcription of nearby genes. Additionally, H3K27ac occupancy also correlates well with gene expression in general apart from at p63 binding sites (median Pearson's R = 0.72) (Fig 2B), which is consistent with previous reports of the correlation of H3K27ac with gene transcription [34]. These findings suggest that p63-regulated gene expression can be predicted by dynamic H3K27ac occupancy at p63 binding sites.

To further investigate the dynamics of H3K27ac occupancy at p63 binding sites, we clustered p63 binding sites into seven groups based on the co-localized H3K27ac signals using K-means clustering (Fig 3A; Supplementary Table S9A). Subsequently, we compared genes associated with these H3K27ac clusters (H3K27ac occupancy clusters in Fig 3B) with those in the nine clusters based on gene body RNAPII occupancy (Fig 1B, RNAPII occupancy clusters in

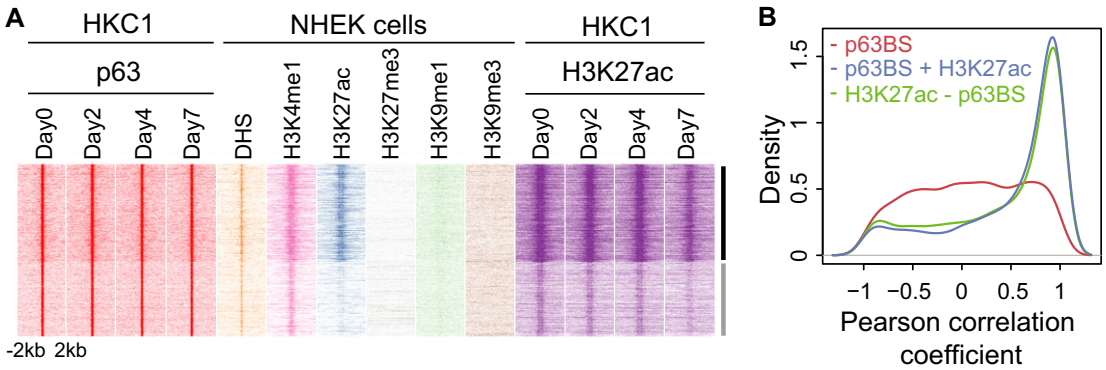

Figure 2. Epigenetic signature of p63 binding sites and correlation of p63 binding with gene regulation in epidermal keratinocytes.

A Heatmap of DNase1 hypersensitivity sites (DHS) and histone modifications (H3K4me1, H3K27ac, H3K27me3, H3K9me1, and H3K9me3) occupancy in NHEK cells (ENCODE), and p63 and H3K27ac occupancy from differentiating keratinocytes at p63 binding sites (genomic regions of a 4-kb window with summits of p63 binding sites in the middle in each panel). The p63 binding sites are categorized in two groups: active p63 binding sites with high H3K27ac signal (indicated with the black bar) and inactive p63 binding sites with low H3K27ac signal (indicated with the gray bar).

B Correlation of p63 binding or H3K27ac at enhancers with transcription of nearby genes during differentiation. Distribution of the Pearson correlation coefficients for ChIP-seq signals at enhancers compared to the RNAPII occupancy of associated transcribed genes during keratinocyte differentiation. Blue line: enhancers marked by H3K27ac that overlap with p63 binding sites; green line: enhancers marked by H3K27ac that do not overlap with p63 binding sites; and red line: p63 signal of p63 binding sites.

Source data are available online for this figure.

 © 2015 The Authors

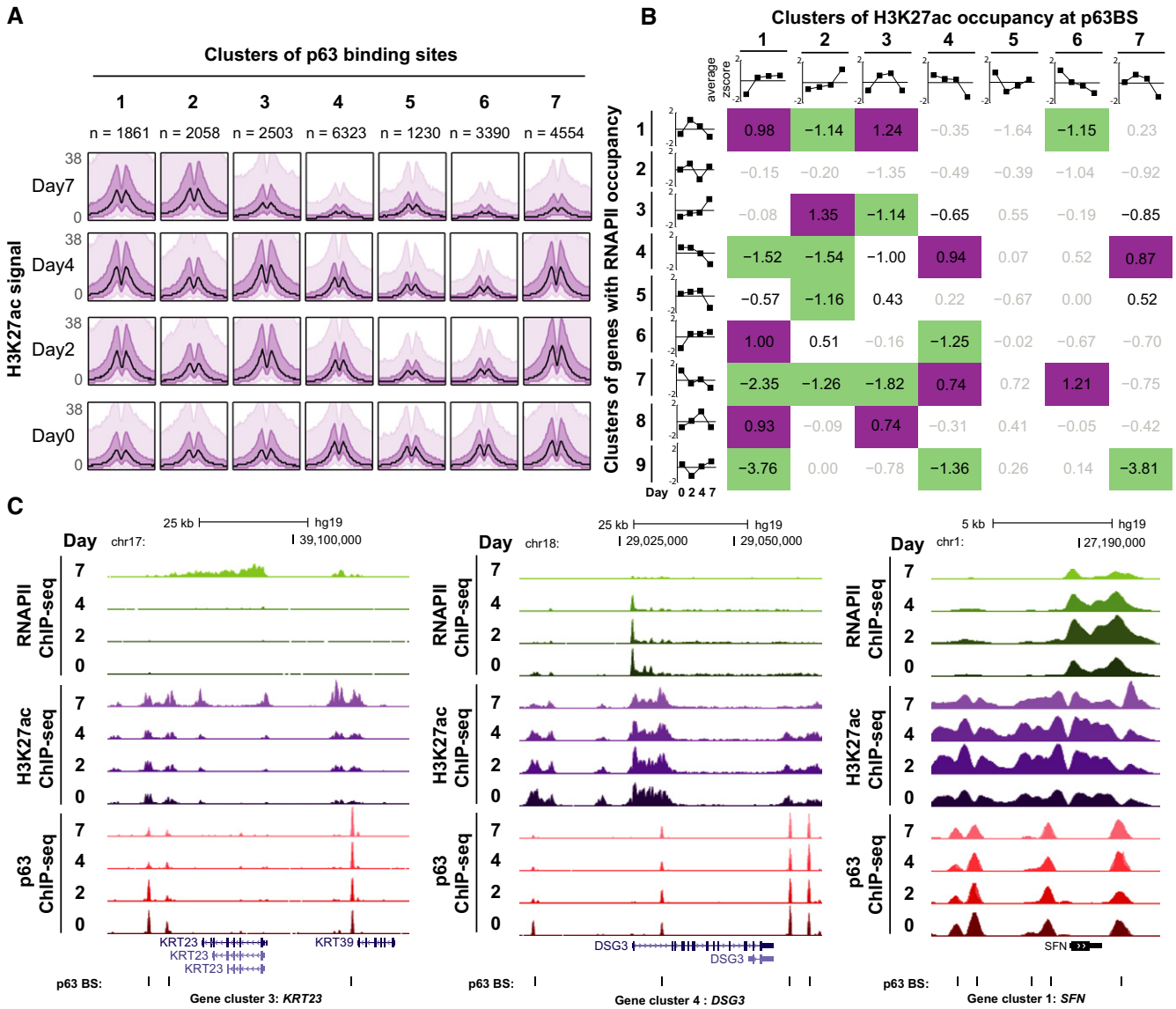

Figure 3. Dynamically regulated active p63 binding sites during epidermal differentiation.

A H3K27ac dynamics at p63 binding sites during epidermal differentiation. p63 binding sites were clustered to seven groups by K-means clustering based on the co-localized H3K27ac signals at the binding sites (genomic regions of a 4-kb window with summits of p63 binding sites in the middle in each panel) during differentiation. The average H3K27ac signal at p63 binding sites in each panel is depicted in black. H3K27ac signal range of 50% and 90% of p63 binding sites is depicted in purple and light purple, respectively. Clusters are arranged along the horizontal axis, stages of differentiation along the vertical axis.

B Over- and underrepresentation of shared genes associated with p63 binding sites clustered based on H3K27ac occupancy dynamics (seven clusters) (Fig 3A) compared with clusters defined by RNAPII occupancy dynamics (nine clusters, Fig 1B) during differentiation. Significant fold enrichments per gene cluster with active p63BS nearby (hypergeometric analysis, *P*-value < 0.001) are depicted in $\log_2$-transformed values (< 0.5-fold (depletion, green box) and > 1.5-fold (enrichment, purple box)); the insignificant associations are depicted in gray text. The graphs on the top illustrate the average H3K27ac occupancy (average *z*-score of $\log_2$ (RPKM)) at p63BS at all four selected time points of keratinocyte differentiation (days 0, 2, 4, and 7) per H3K27ac cluster. The graphs depicted on the left show the average signal (average *z*-score of $\log_2$ (RPKM)) of RNAPII at the 4 days of keratinocyte differentiation (days 0, 2, 4, and 7) per gene cluster.

C Screenshot from UCSC genome browser of normalized RNAPII ChIP-seq (green), H3K27ac ChIP-seq (purple), and p63 ChIP-seq (red) signals at *KRT23*, *DSG3*, and *SFN* loci. Examples of genes from specific RNAPII gene clusters that show positive correlation of dynamic H3K27ac signals at nearby p63 binding sites with the gene transcription patterns during keratinocyte differentiation; *KRT23* (gene cluster 3) with p63 peaks (H3K27ac cluster 2), *DSG3* (gene cluster 4) with p63 peaks (H3K27ac clusters 4 and 7), *SFN* (gene cluster 1) with p63 peaks (H3K27ac clusters 1 and 3).

Source data are available online for this figure.

Fig 3B), to assess the correlation between the H3K27ac occupancy at the p63 binding sites and transcription of the nearest genes. We observed that RNAPII and H3K27ac clusters with similar dynamics shared more genes than expected, while those with divergent dynamics shared fewer genes than expected (Fig 3B). For example, genes associated with H3K27ac cluster 2 with increased H3K27ac

© 2015 The Authors

signal are enriched for genes present in RNAPII cluster 3 that show increased expression during late differentiation (e.g., *KRT23*) (Fig 3B and C; Supplementary Tables S1A and S9A and B). In contrast, genes associated with H3K27ac cluster 2 are depleted for genes present in RNAPII clusters 1, 4, 5, and 7, all of which show decreased expression during differentiation (e.g., *DSG3*) (Fig 3B and C; Supplementary Tables S1A and S9A and B). Genes associated with H3K27ac cluster 3 with first increased and then decreased H3K27ac signal are enriched for genes from RNAPII cluster 1 that show similar dynamics (e.g., *SFN*) (Fig 3B and C; Supplementary Tables S1A and S9A and B).

Taken together, both general and per-cluster correlation analyses of RNAPII and H3K27ac occupancy indicate that H3K27ac signal at p63 binding sites rather than p63 binding signal alone is informative for the prediction of the transcriptional program regulated by p63 and that assessing H3K27ac occupancy at p63 binding sites could facilitate the identification of p63 target genes in keratinocytes.

Potential co-activators of p63

As p63 binding alone does not explain epidermal gene expression, we searched for potential p63 co-regulators by transcription factor motif enrichment analysis using position weight matrices (PWM) of known transcription factor family motifs (threshold, *P*-value = 0.01, 1.5-fold enrichment versus background) [35]. An enrichment of motifs from the ZFX, RUNX, and EBF1 families was detected in active p63 binding sites with the H3K27ac mark (Fig 4A; Supplementary Tables S7 and S8A). Among transcription factors that can bind to these motifs, *RUNX1* is expressed in proliferating and differentiating keratinocytes (Supplementary Fig S5B; Supplementary Table S7). ChIP-qPCR analysis showed that RUNX1 was indeed bound to a number of tested p63 binding sites with the RUNX motif (Fig 4B; Supplementary Table S8B), indicating that RUNX1 can cooperate with p63 in epidermal cells. For "inactive" p63 binding sites that were not co-localized with the H3K27ac mark, an enrichment of the NR2 nuclear receptor family motif was found (Fig 4A; Supplementary Table S7), and among transcription factors that can bind to this motif, *RXRA* is expressed in keratinocytes. Some motifs were enriched in both active and inactive p63 binding sites. For example, a strong enrichment of the motif sequence bound by the p53 family proteins including p63 was detected (Supplementary Table S7). This is consistent with the high percentage of p63 motif-containing p63 binding sites detected by p63scan (90%). Other motifs that were enriched in both active and inactive binding sites include the motif of TFAP2α that has been reported to be a co-regulator of p63 (Supplementary Table S7). TFAP2α binding to p63-bound regions in keratinocytes was confirmed by ChIP-qPCR (Fig 4B; Supplementary Table S8C).

To search for potential p63 co-regulators during specific stages of epidermal stratification, we determined motif enrichment in the seven clusters of p63 binding sites that show differential H3K27ac occupancy patterns during differentiation. Several transcription factor family motifs were enriched in specific clusters, for example, FOXQ1 in H3K27ac cluster 1, MAFB and SP100 in cluster 2, E2F in cluster 5, and VDR in cluster 6 (Fig 4C; Supplementary Table S9C). Although the precise function of these transcription factors in epidermal stratification is not yet clear, it is likely that they cooperate with p63 in keratinocyte differentiation as they have been shown to regulate cell proliferation and differentiation [36–40].

Clustered p63 binding sites (cl-p63BS) and clustered epidermal enhancers

Clustered enhancers, also referred to as super-enhancers, are defined as stretches of active enhancers that are bound by high levels of lineage-specific master transcription factors and co-activators that drive gene expression to define cell lineage identity [41,42]. The essential role of p63 for the commitment to the epithelial lineage has been well established, and it is likely that p63 binds to clustered enhancers. Therefore, we investigated whether p63 can bind to clustered enhancers for its function in epithelial lineage determination. We observed an enrichment of clusters of five or more p63 binding sites (hypergeometric test, *P*-value = 9.06E-13) within 100 kb of the transcription start site of transcribed genes (RNAPII occupancy, *RPKM* > 1) relative to all genes (Supplementary Table S10). We subsequently performed analyses using an established algorithm for detecting clustered enhancers [42] on two of our datasets: on p63 ChIP-seq data to identify regions with clustered p63 binding sites with high p63 binding signals, referred to as clustered p63 binding site regions (cl-p63BS) (Supplementary Table S14A), and on H3K27ac ChIP-seq data to identify regions with clustered H3K27ac-marked enhancers. Regions with clustered H3K27ac-marked enhancers have been reported to drive cell-type-specific gene expression [42,43] and are therefore referred to as clustered epidermal-specific enhancers (cl-epidermal enhancers) hereafter (Supplementary Table S11A). Our analyses identified 1,293 cl-epidermal enhancers (Fig 5D and E) and 1,991 regions as cl-p63BS (Fig 5E). Of all 1,293 identified cl-epidermal enhancers, 1,182 (91.4%) sites overlapped with at least one p63 binding site (Fig 5A and D). In addition, p63 preferentially binds to cl-epidermal enhancers (clustered H3K27ac-marked enhancers) rather than to single active enhancers (single H3K27ac peaks) and random controls (hypergeometric test and normal distribution probability test, respectively, *P*-value < 1E-323 in all cases) (Fig 5A). Three p63 binding sites on average were identified within each cl-epidermal enhancer, whereas randomized control sets contained zero p63 binding sites on average (Fig 5B). These observations show that p63 binding sites are enriched in cl-epidermal enhancers in epidermal keratinocytes, and underscore the importance of p63 as a key transcription factor in epithelial lineage commitment. Out of a total number of 1,991 cl-p63BS, 617 share genomic regions with 589 cl-epidermal enhancers out of a total number of 1,293 (Fig 5E) and are hereafter considered as active epidermal cl-p63BS (Supplementary Table S15A and B). Interestingly, approximately two-thirds of the cl-p63BS do not overlap with active cl-epidermal enhancers. Next, we used K-means clustering to identify six gene clusters associated with cl-epidermal enhancers showing different patterns of H3K27ac occupancy during differentiation (Fig 5C; Supplementary Table S11A). These clusters were enriched for genes with concordant RNAPII occupancy patterns during differentiation and depleted for genes with discordant RNAPII differentiation dynamics (Fig 5C). Compared to the association of single p63-bound enhancers with gene expression (Fig 3B), these p63 binding site-containing cl-epidermal enhancers showed higher fold enrichment of gene clusters with similar expression patterns (Fig 5C). In summary, our data showed that p63 binds to clustered enhancers, consistent with the role of p63 in epithelial commitment, and that these clustered enhancers play roles not only in epithelial commitment but also during epidermal differentiation.

 © 2015 The Authors

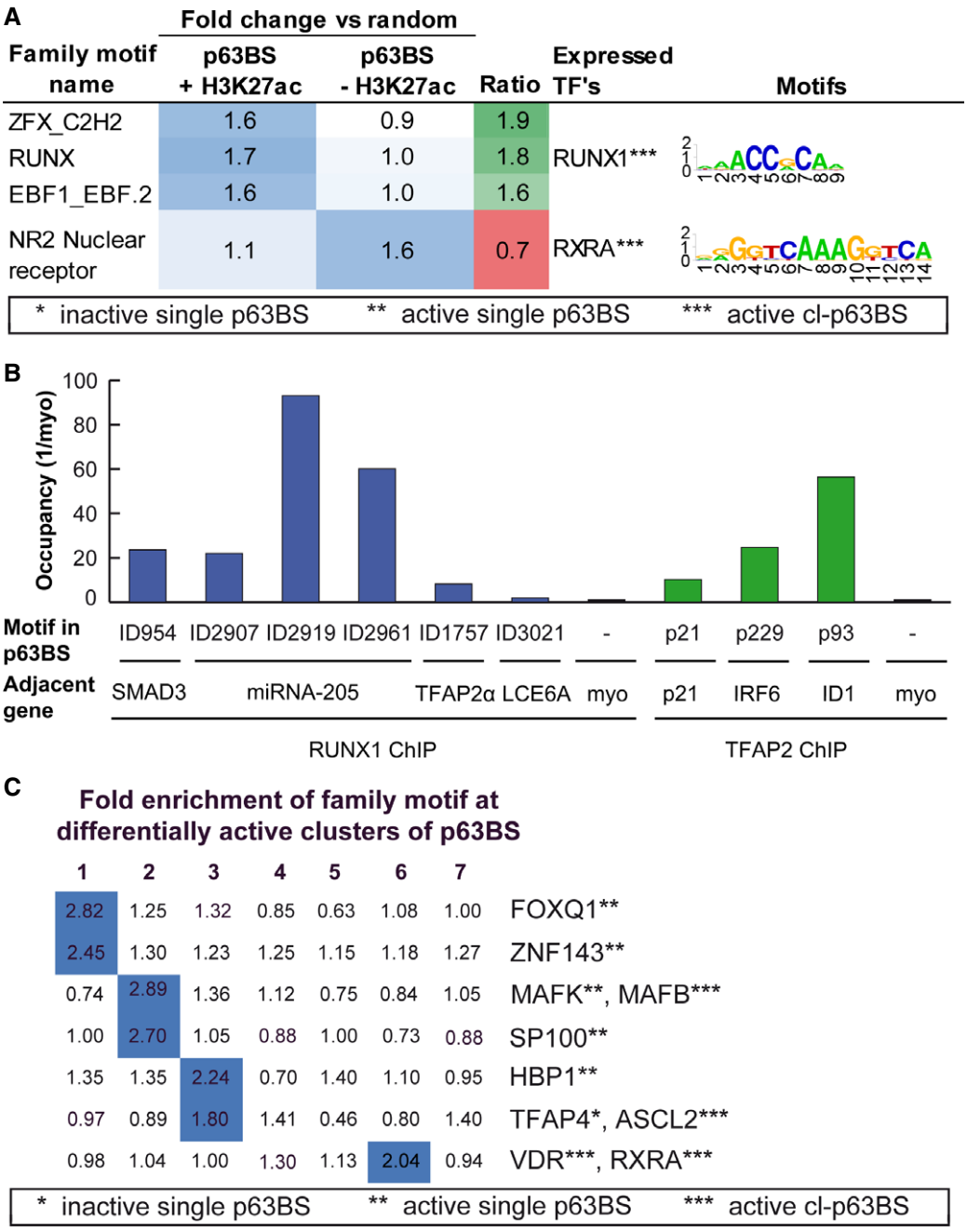

Figure 4. Cofactors of p63 in epidermal keratinocytes.

A Differential enrichment (in blue boxes, threshold, *P*-value = 0.01, 1.5-fold enrichment versus background) of transcription factor binding motifs in active or inactive p63 binding sites as compared to random sites. Only the enriched motifs in either active or inactive p63 binding sites with a fold change ratio ($\log_2$) of > 1.5 and < 0.7 are shown. The transcription factors (TF) that can bind to these motifs and are expressed in keratinocytes, RUNX1 and RXRA, and the corresponding binding motif sequences are indicated on the right (Supplementary Table S7). Both RUNX1 and RXRA have at least one p63 binding site nearby indicated by the asterisks, *** with active cl-p63BS.

B ChIP-qPCR analysis of RUNX1 and TFAP2α binding to p63 binding sites. Specific binding of RUNX1 was observed at p63 binding sites near active genes *SMAD3*, *miRNA-205*, and *TFAP2α*. Low RUNX1 binding was also detected at the p63 binding site near *LCE6A*, but not at the negative control region myoglobin exon 2 (myo). Specific binding of TFAP2 was observed at p63 binding sites near *p21*, *IRF6*, and *ID1*, but not at the negative control region myo. Occupancy represents the fold enrichment of the percentage of input DNA at the target region over that at the negative control region myo. This ChIP-qPCR analysis (n = 1) was confirmed by other independent experiments (data not shown).

C Fold enrichment of transcription factor binding motifs in each of the seven dynamically regulated active p63 binding site clusters (Fig 3A). The corresponding transcription factors that can bind to these motifs and are expressed in keratinocyte are indicated on the right (Supplementary Table S9C). All these transcription factors have at least one p63 binding site nearby indicated by the asterisks, * with inactive p63 binding sites, ** with active single p63 binding sites, or *** with active cl-p63BS.

© 2015 The Authors

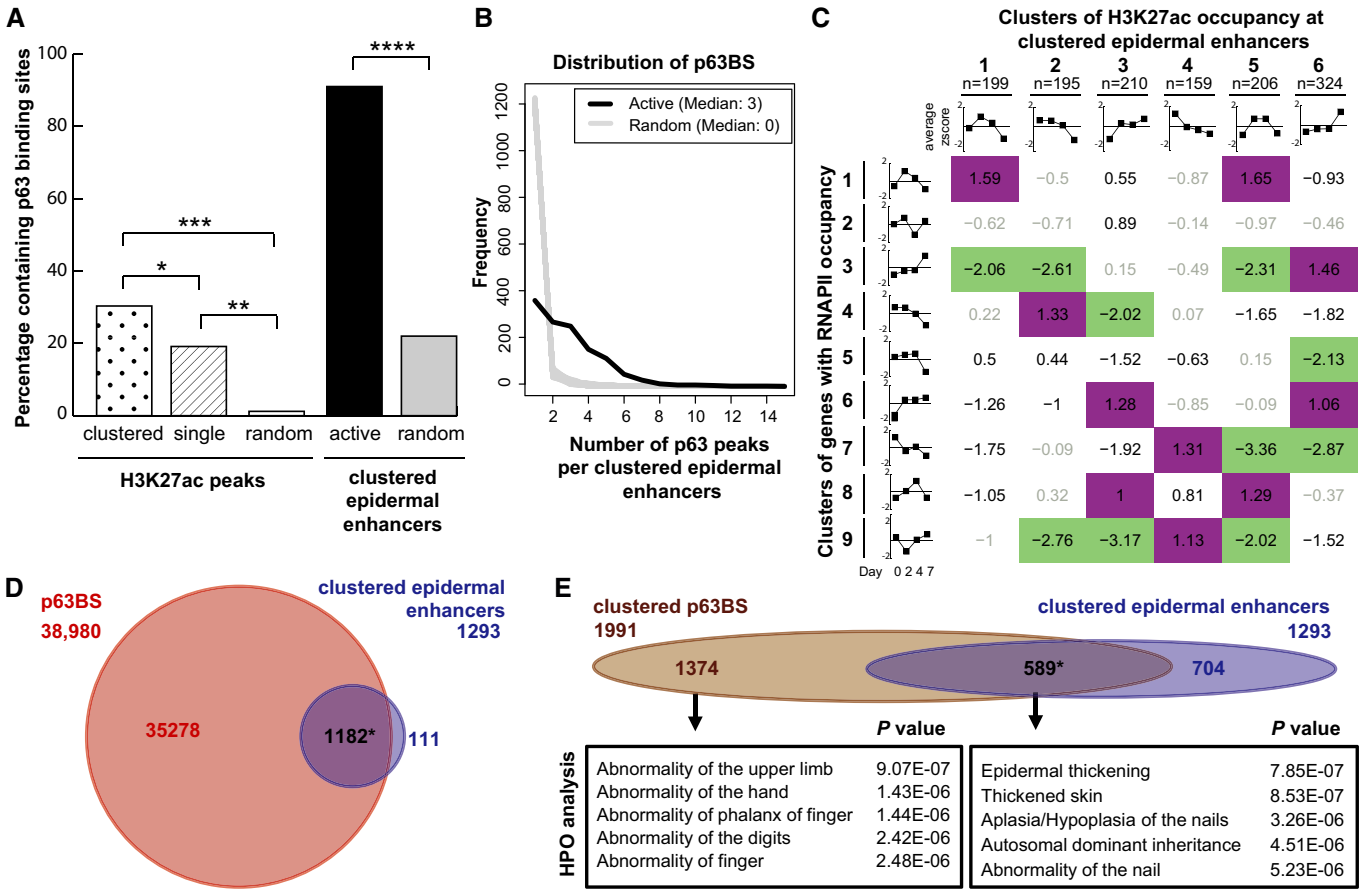

Figure 5. p63 binding sites (p63BS), clustered p63 binding sites (cl-p63BS), and clustered epidermal enhancers (cl-epidermal enhancers) in gene regulation.

A Percentage of individual H3K27ac peaks that contain at least one p63 binding site in cl-epidermal enhancers (genomic regions with clustered H3K27ac signals, dotted), single enhancers (single H3K27ac peak, diagonal stripes), and a control set of randomly shuffled single enhancers (white) (hypergeometric analysis, **P*-value < 1E-323, ***P*-value < 1E-323, ****P*-value < 1E-323). The rightmost two bars show the percentage of cl-epidermal enhancers that contain at least one p63 binding site (black) compared to the mean percentage of 1,000 randomly shuffled control sets (gray) (SE = 0.001%) (*****P*-value < 1E-323; calculated from normal distribution fitted to the random control percentages, which are normally distributed (Shapiro–Wilk normality test *P*-value = 0.52)).

B Distribution of the number of p63 peaks per cl-epidermal enhancer (black) and 1,000 randomized controls (gray).

C Over- and underrepresentation of shared genes associated with cl-epidermal enhancers clustered based on H3K27ac occupancy dynamics (six clusters) compared with clusters of genes defined by RNAPII occupancy dynamics (nine clusters, Fig 1B) during keratinocyte differentiation. Significant fold enrichments (hypergeometric analysis, *P*-value < 0.001) are depicted in $\log_2$-transformed values (< 0.5-fold (depletion, green box) and > 1.5-fold (enrichment, purple box)); not significant associations are depicted in gray text. The graphs on the top illustrate the average H3K27ac occupancy at p63BS at all four selected time points of keratinocyte differentiation (days 0, 2, 4, and 7) per H3K27ac cluster. The graphs depicted on the left show the average signal of RNAPII at the 4 days of keratinocyte differentiation per gene cluster.

D Overlap of individual p63 binding sites and cl-epidermal enhancers. Of a total number of 38,980 p63 binding sites (red), 35,278 lie outside the cl-epidermal enhancers. Majority of the cl-epidermal enhancers (1,182 (*) of 1,293, blue) contains at least one p63 binding site (red). Only 111 cl-epidermal enhancers do not contain any p63 binding site (blue).

E Overlap of cl-epidermal enhancers (blue) and cl-p63BS (brown). 617 cl-p63BS out of a total number of 1,991 and 589 (*) cl-epidermal enhancers out of a total number of 1,293 share genomic regions, and these regions are referred to as active cl-p63BS. A proportion of cl-p63BS (1,474) do not overlap cl-epidermal enhancers, while 704 cl-epidermal enhancers do not overlap cl-p63BS. Human Phenotype Ontology (HPO) analysis of genes near active cl-p63BS and cl-epidermal enhancers shows enrichment for genes associated with skin phenotypes, whereas HPO analysis of those near inactive cl-p63BS shows enrichment for genes associated with defect in other epithelial-related developmental processes. Complete data summarized in Supplementary Tables S11, S14, S15, S16 and S17.

Source data are available online for this figure.

p63-regulated genes and their relevance to disease

Knockdown or knockout of *p63* in epithelial cells to identify de-regulated genes [14,17] has been the major approach in previous p63 target gene studies. The main drawback of this approach is that loss of p63 results in epithelial differentiation defects, and genes that are expressed at a later stage of differentiation and regulated by p63 may not be identified. In this study, we took a different approach and used differentiating normal keratinocytes. To identify p63 target genes, we first associated all identified p63 binding sites (38,980) with their nearest gene (11,890) (Supplementary Table S12A) and analyzed gene function using DAVID Gene Ontology annotation [24]. This showed an enrichment of genes involved in intracellular signaling cascade, phosphorylation, vascular development, cell

 © 2015 The Authors

migration, and cell death (Supplementary Table S12B). Altogether, 10,020 p63 binding sites were identified in the proximity of differentially regulated genes (RNAPII ChIP-seq clusters, *RPKM* > 1) during epidermal differentiation and 74.2% of these binding sites are co-localized with H3K27ac (Supplementary Table S1D). These differentially regulated genes with active p63 binding sites nearby were considered potential p63 target genes (1,961 based on RNAseq and 2,760 based on RNAPII) (Supplementary Tables S1D and S2D). For example, p63 binding sites with increasing levels of the H3K27ac mark during differentiation were observed near the *IVL*, *LCE1B*, and *LCE1C* genes that are highly expressed in late differentiating keratinocytes (Supplementary Fig S5C). Several of these potential p63 target genes are known to be causative genes involved in epidermal diseases, such as *CDH3, DSG1, KRT5, KRT10,* and *FLG* (Supplementary Fig S5C; Supplementary Table S13A and B) [10,11,44–46]. Of note, many of these potential p63 target genes such as *KRT1* and *PRDM1* were not previously considered as direct p63 target genes (Supplementary Fig S5D; Supplementary Table S13A–D). Furthermore, we compared the potential p63 targets identified in this study with previous p63 RNAi knockdown experiments (Supplementary Table S13C) [14,17]. Among the 120 p63-regulated genes previously reported in two p63 RNAi knockdown experiments [14,17], we found that 70 of them (57.5%) are among potential direct p63 targets in this study (Supplementary Table S13D). Interestingly, many co-regulators of p63 including RUNX1 [47], VDR [48], RXRA [49], and FOXQ1 in epidermal keratinocytes are either known p63 targets genes or identified as potential p63 targets in this study (Fig 4A and C). Taken together, our data show that p63 targets are expressed in different layers of the epidermis and associated with distinct disease phenotypes (Supplementary Fig S2B).

Intriguingly, p63 binding sites were also identified in the vicinity of 80 pri-miRNAs of the 130 pri-miRNAs that are differentially regulated during keratinocyte differentiation (Supplementary Fig S3A; Supplementary Table S4B). Among these pri-miRNAs, 74 of them contain at least one p63 binding site with H3K27ac occupancy, including pri-*miR-203* and pri-*miR-205* (Supplementary Fig S3B; Supplementary Table S4B), which suggests that these miRNAs are targets of p63. Among these p63-regulated miRNA genes, *miR-205* is a known p63 target [50,51]. Another potential p63-regulated miRNA is *miR-203* that is known to regulate *p63* at the mRNA level during keratinocyte differentiation [30], and thus, our data suggest a regulatory feedback loop of p63 and *miRNA-203* during differentiation.

In comparison with genes mapped to single p63 binding sites, genes mapped to the 1,991 cl-p63BS (clustered p63 binding sites) (Fig 5E) showed a stronger enrichment of genes involved in ectoderm and epithelium development (Supplementary Table S14A–D). This may be due to genes in the vicinity of cl-p63BS being more likely to be true p63 target genes compared with those near single p63 binding sites. Genes associated with nearby cl-epidermal enhancers (clustered epidermal enhancers marked by H3K27ac) (Fig 5D and E) are enriched for genes with epidermal-related functions (Supplementary Table S11C). Genes mapped to these active epidermal cl-p63BS (overlap of cl-p63BS and cl-epidermal enhancers) likely play a role in epidermal development (Supplementary Table S15C), similar to genes mapped to cl-epidermal enhancers (Supplementary Table S11C). Human Phenotype Ontology (HPO) analysis showed that this group of genes including *CLDN1*, *p63*, and *KRT17* are associated with skin-related abnormalities such as epidermal thickening, aplasia/hypoplasia of the nails, and hyperkeratosis (Fig 5E; Supplementary Table S15D). Genes in the vicinity of cl-epidermal enhancers that do not overlap cl-p63BS were enriched with genes that play a role in epidermal development (Supplementary Table S16C), similar to the genes that were mapped by all cl-epidermal enhancers (Supplementary Table S11C). In contrast, the 69% of cl-p63BS that do not overlap cl-epidermal enhancers mapped to genes with broader functions including regulation of cell proliferation, tube development, vascular development, and regulation of apoptosis (Supplementary Table S17D). HPO analysis revealed that these genes are associated with epithelial-related non-skin phenotypes such as limb and tooth defects (Fig 5E; Supplementary Table S17D), suggesting that inactive enhancers regulate gene expression during the development of other epithelial-related structures.

Discussion

Tightly regulated gene expression during epidermal differentiation is crucial for the establishment and maintenance of the epidermis, and therefore, it is essential to obtain a complete gene regulatory map to understand the biology of the epidermis and related diseases. Here, we report an atlas of differentially expressed genes during epidermal differentiation and regulatory regions that are bound by p63, a key regulator in epidermal differentiation. We show that the activity of p63 binding sites as defined by co-localized H3K27ac signals, rather than p63 binding itself, correlates with the expression of nearby genes. Many of these epidermal genes are associated with distinct skin disease phenotypes and likely regulated by p63. Furthermore, our data show that not all p63 binding sites are active and suggest that the p63 binding sites that are "inactive" during keratinocyte differentiation are active and regulate genes in other epithelial tissues during different stages of development, and are relevant to epithelial-related diseases.

In this study, we used an established keratinocyte differentiation model [16]. Expression of epidermal marker genes shown by the individual gene approaches such as RT–qPCR analysis (Supplementary Fig S1B and C) and by the RNAPII ChIP-seq and by RNA-seq profiling approaches (Fig 1A, Supplementary Fig S1A) is consistent with the expression of these genes *in vivo* [20,21]. These data confirm previous reports that this differentiation model under submerged condition allows the expression of genes that are normally found in the differentiating epidermis [16,20,52].

The genomewide unbiased RNAPII ChIP-seq and RNA-seq profiling approaches not only revealed the global expression dynamics but also provided information that is not easily obtained by specific gene approaches, such as the expression of gene isoforms and transcription of miRNAs. Our RNAPII ChIP-seq and RNA-seq data at the *TP63* gene locus showed that Δ*Np63* is the main isoform during keratinocyte differentiation, whereas the expression of the *TAp63* isoform was not detected (Supplementary Fig S1D). These data are consistent with results from a recent RNA-seq analysis of the developing mouse epidermis [53] and from p63 isoform-specific knockout experiments that demonstrated the major functional role of ΔNp63 in the epidermis [54,55]. These observations do not however rule out the possibility that the TAp63 isoform is expressed at an extremely low level, and the expression might be detected with deeper

© 2015 The Authors

sequencing. So far, studies on the biogenesis of miRNAs have mainly been focused on processing of pri-miRNAs to miRNAs [56, 57], while data on transcriptional regulation of miRNA genes are limited. We show that RNAPII ChIP-seq analysis enables the detection of pri-miRNA transcription (Supplementary Fig S3A; Supplementary Table S4A) [29]. Many of these miRNAs are known to have a role in epidermal differentiation such as *miR-205* and *miRNA-203* (Supplementary Fig S3B) [27,30,31]. In combination with our p63 and H3K27ac ChIP-seq analyses, some of these miRNAs are identified as potential direct p63 targets, as they have an active p63 binding site with the co-localization of H3K27ac nearby (Supplementary Fig S3B; Supplementary Table S4B).

Our data showed that approximately half of all identified p63 binding sites were co-occupied by H3K27ac and are considered as active binding sites (Fig 2A). Consistently, about one-third of cl-p63BS (stretches of p63 binding sites) share genomic regions with cl-epidermal enhancers (stretches of H3K27ac sites) (Fig 5E) and are considered as active epidermal cl-p63BS. These data suggest that p63 binding alone is not sufficient for the regulation of gene transcription, and indeed, gene expression dynamics correlates better with the H3K27ac signal at p63 binding sites than with p63 binding itself (Fig 2B). This suggests the involvement of other co-regulators in p63 gene regulation during differentiation. Indeed, our analyses of transcription factor motif enrichment and ChIP-qPCR experiments showed that RUNX1 potentially cooperates with p63 at active p63 binding sites in keratinocytes (Fig 4A and B). In contrast, p63 binding sites that are not co-localized with the H3K27ac mark were enriched for the NR2 nuclear receptor family motif that can be bound by RXR family proteins (Fig 4A), suggesting that these proteins may function as repressors at p63 binding sites in keratinocytes. Other co-regulators seem to play a role in cooperating with p63 to regulate dynamic gene expression during keratinocyte differentiation (Fig 4C). Interestingly, some of these identified p63 co-regulators are known or potential p63 targets (Fig 4A and C), suggesting that p63 regulates the expression of these co-regulators and that these co-regulators cooperate with p63 to regulate its target genes, which is consistent with the role of p63 as a master regulator in epithelial cells.

The absence of dynamic p63 binding during epidermal differentiation in keratinocytes is distinct from the induced binding of lineage-specific transcription factors during early embryogenesis [58] and differentiation of embryonic stem cells into specific lineages [59]. A plausible explanation is that epidermal keratinocytes are a type of established epithelial cells, and differentiation of this type of multipotent stem cells might require different gene regulation mechanism compared to that in pluripotent embryonic stem cells or in early embryogenesis. It should be noted that our analyses do not discriminate whether p63 acts as an activator or a repressor factor; especially for genes with "inactive" p63 binding sites (without H3K27ac signal) nearby, p63 may function as a repressor. However, it is unlikely that p63 recruits repression complexes such as polycomb proteins or induces heterochromatin formation, as p63 binding sites are co-localized with open chromatin regions marked by DHS and with enhancer marks such as H3K4me1 but are not co-localized with H3K27me3 and H3K9me3 marks (Fig 2A). One scenario is that the binding of p63 may mark epithelial lineage-related regulatory elements as a placeholder during epithelial commitment, and the recruitment of different sets of co-regulators is required for gene regulation in an epithelial-related tissue- and stage-specific manner. This hypothesis is supported by previous reports that p63 binding sites identified in epidermal keratinocytes have been found to be associated with limb and palate development and with relevant diseases, split hand/foot malformation [18] and van der Woude syndrome where cleft lip/palate is one of the major features [60,61]. The placeholder paradigm of transcription factor-mediated regulation has been reported for a group of transcription factors such as FoxA and GATA proteins in lineage progenitor cells [62]. These transcription factors are the first factors to engage in enhancers during development, and their expression is required for lineage establishment.

In summary, we provide an expression atlas of epidermal genes including non-coding RNAs during epidermal differentiation, as well as a catalog of p63-regulated genes and regulatory regions that are bound by p63, a key regulator in epidermal differentiation. We show that the activity of p63 binding sites as defined by co-localization of histone modification mark H3K27ac signals correlates with the expression of nearby genes. Many of these epidermal genes are associated with distinct skin disease phenotypes. Among these p63-regulated genes, those that are not yet associated with skin diseases can be used as candidate causative genes for genetic studies such as the prioritization of exome sequencing data. The catalog of p63-regulated enhancers and clustered epidermal enhancers may provide potential genomic regions to study causative variants or genetic modifiers in non-coding regions and to elucidate the heterogeneity of sub-phenotypes of skin diseases. Importantly, we show that not all p63 binding sites are active in gene regulation in epidermal cells. This suggests that the p63 binding sites that are "inactive" during keratinocyte differentiation are active and regulate genes in other epithelial tissues during different stages of development. These "inactive" p63 binding sites may be relevant to other p63-related diseases. We propose that the transcription factor p63 serves as a placeholder and bookmarks enhancers that can regulate gene expression at different stages and in different tissues during development. It will be of interest to investigate whether p63 occupies genomic loci in a passive manner or actively shapes chromatin accessibility during epithelial lineage commitment.

Materials and Methods

Ethics statement

All procedures regarding establishing human primary keratinocytes were approved by the ethics committee of the Radboud University Nijmegen Medical Centre ("Commissie Mensgebonden Onderzoek Arnhem-Nijmegen"). Informed consent was obtained.

Human primary keratinocyte culture

Skin biopsies were taken from the abdomen of two healthy volunteers to set up the primary keratinocyte culture, referred to as HKC1 and HKC2 [63]. Keratinocyte cultures in keratinocyte growth medium (KGM) under undifferentiated condition were previously described [64], and differentiation of keratinocyte cultures was induced by cell contact inhibition and excluding

 © 2015 The Authors

several growth factor supplements: bovine pituitary extract (Bio Whittaker), EGF (Sigma), insulin (Sigma), and hydrocortisone (Calbiochem) from the medium. The medium was changed every second day, and before harvesting of the RNA and chromatin. Cells were collected on day 0, and on days 2, 4 and 7 after induction of differentiation.

ChIP and ChIP-seq

Human primary keratinocytes under proliferating, early, mid-, and late differentiation condition generated from HKC1 were used for ChIP and ChIP-seq analysis. ChIP-sequencing datasets were generated with an antibody recognizing the alpha isoforms of p63 (H129, Santa Cruz), an antibody that detects all forms of the large subunit of RNA polymerase II (8WG16, Santa Cruz), and a H3K27ac antibody recognizing the acetylation of the lysine 27 residue of histone H3 (H3K27ac, C15410174, pAb-174-050, Diagenode). ChIP-qPCR experiments were performed using 2 μg RUNX1 antibody (ab23980, Abcam) and 1 μg TFAP2 antibody (C18X, Santa cruz). RNAPII, p63, H3K27ac, RUNX1, and TFAP2 ChIP experiments were performed as previously described [65], with a minor change of using magnetic beads (Novex by Life Technologies, 10008D and 10009D).

RNA extraction and RNA-seq

Human primary keratinocytes under proliferating, early, mid-, and late differentiation condition were used for RNA-seq analysis. RNA extraction was carried out using the NucleoSpin RNA II kit (740,955.50; MACHEREY-NAGEL, Düren, Germany). cDNA synthesis from 1 μg total RNA as control for RNA-seq was carried out using the iScript cDNA synthesis kit (Bio-Rad; 170-8891, CA, Hercules, USA). Starting amount of RNA-seq sample was 1 μg, and rRNA was depleted using the Ribo-Zero rRNA Removal Kit (Human/Mouse/Rat; MRZH11124, Epicentre, Madison, WI, USA) according to the manufacturer's instructions. RNA fragmentation reactions were performed using fragmentation buffer (5×; 200 mM Tris-Ac, 500 mM potassium-Ac, 150 mM magnesium-Ac) in a final concentration of 1× per reaction. Each 50-μl fragmentation reaction was incubated at 95°C for 1.5 min on a thermal cycler and placed on ice for 10 min. Ethanol precipitation was used to purify the reactions. The fragmented rRNA-depleted RNA was combined with 5 μg of random hexamers (Roche) in a final volume of 11 μl, incubated at 65°C for 5 min, and afterwards immediately placed on ice. The remaining reagents were added to the reaction: 4 μl 5× first-strand buffer (Invitrogen), 2 μl DTT (0.1 M Invitrogen), 1 μl dNTP mix (10 mM Invitrogen), 2 μl actinomycin D (0.1 μg/μl Sigma), 1 μl of RNase H (40 U/ml Ambion), and 1 μl SuperScript III (200 U Invitrogen). The first-strand reaction was incubated at 25°C for 10 min, 50°C for 90 min, followed by deactivation at 70°C for 15 min, followed by MinElute Reaction Cleanup Kit (Qiagen), according to the manufacturer's protocol. The second strand was synthesized by adding 20 μl 5× second-strand buffer (Invitrogen), 4 μl 5× first-strand buffer (Invitrogen), 2 μl DTT (0.1 M Invitrogen), 1 μl random hexamers (5 mg/ml Roche), dUTP mix (12.5 mM Invitrogen), 1 μl RNase H (8 U/ml Ambion), 1 μl *E. coli* DNA polymerase I (10 U/μl Invitrogen), and 1 μl *E. coli* DNA ligase (10 U/μl NEB) to the purified sample (100 μl total volume). After 2 h at 16°C, 1 μl of T4 DNA polymerase (10 U/μl Promega) was added and the reaction was incubated at 16°C for 10 min. The ds-cDNA was purified using the MinElute Reaction Cleanup Kit (Qiagen), according to the manufacturer's protocol.

Illumina library preparation

DNA samples were prepared for sequencing by end repair of 6 ng total DNA (H129 ChIP-seq and RNAPII ChIP-seq samples), 10 ng total DNA (H3K27ac ChIP-seq samples), and 5 ng total cDNA (RNA-seq samples) as measured by Qubit (Invitrogen). Adaptors were ligated to the DNA fragments, followed by a pre-PCR of 4 cycles, size selection ($\sim$300 bp), and subsequently 11 cycles of PCR amplification. Cluster generation and sequencing (50 bp) was performed with the hiSeq Solexa Genome analyzer according to standard Illumina protocols.

Quantitative real-time (qRT–PCR)

Quantitative PCR primers were designed using Primer3 (http://frodo.wi.mit.edu), and qPCRs were performed in the CFX96 Real-Time system (C1000 Touch-Thermal Cycler, Bio-Rad) by using GoTaq qPCR mix (Promega) according to the manufacturer's protocol. For qPCR of cDNA analysis, human acidic ribosomal protein (hARP) was used as a housekeeping gene to normalize the amount of cDNA. Differences in the expression of each gene during differentiation (relative expression) were calculated by $2^{\Delta\Delta Ct}$ method [66]. For qPCR of ChIP analysis, one primer set was used for each tested binding region (Supplementary Table S18) and ChIP efficiency of each binding site was calculated by comparison of the percentage of ChIPped DNA against input chromatin to this percentage at a negative control region. Validation experiments were performed by RT–qPCR with primers (Biolegio BV, Nijmegen, the Netherlands) as shown in Supplementary Table S18.

ChIP-seq data analysis

All 50-bp sequence reads were uniquely mapped to the human genome NCBI build 37 (hg19) using bwa 0.6.1 with standard parameters [67] (Supplementary Table S19). All p63, H3K27ac, and RNAPII ChIP-seq datasets were normalized to the same sequencing depth by randomly removing aligned reads. Duplicated reads were removed before normalization. Peak recognition for p63 ChIP-seq and RNAPII ChIP-seq datasets was performed using MACS2, an updated version of MACS [68] that is specifically designed to process mixed signal types (https://github.com/taoliu/MACS) with default settings and a *P*-value threshold of 1E-9 using a genomic DNA as background control, and results are summarized in Supplementary Table S19. Peaks were mapped to RefSeq genes, downloaded from UCSC Genome Browser (hg19), to determine genomic location of the p63 binding sites at promoter regions (defined as 5 kb upstream of the transcription start site and the end of the first intron of genes), intragenic, intergenic, or 25 kb away from the transcription start site of the gene. Peak recognition for the H3K27ac ChIP-seq dataset was performed using MACS2 using default settings for broad peak calling and a *P*-value threshold of 1E-9 using a genomic DNA as

© 2015 The Authors

background control, and results are summarized in Supplementary Table S19. The identified p63 peaks (38,980) that overlap with the identified H3K27ac peaks by MACS2 are considered active p63 binding sites (22,190), while those that do not overlap the MACS2-detected H3K27ac peaks are considered inactive p63 binding sites (16,790).

RNA-seq data processing

All 50-bp single-end RNA-seq reads from two keratinocyte cell lines (biological replicates) were mapped to the human genome NCBI build 37 (hg19) using gsnap version 2013-03-31 [69]. The generated data per condition are summarized in Supplementary Table S19. Spliced reads were mapped using the Ensembl 68 reference transcriptome [70]. Transcript quantification and differential expression analysis were done with cufflinks and cuffdiff v2.1.1 [71], using the RefSeq transcriptome [72], downloaded from the UCSC genome browser website [73] in June 2013.

RNA-seq clustering

RNA-seq RefSeq genes were filtered for those determined to be differentially expressed in at least one comparison by cufflinks/cuffdiff (P-value < 0.05, beta negative binomial model). These were filtered for genes with RPKM expression level of at least 10 in at least one condition, resulting in a set of 3,639 distinct genes, and 3,813 when considering different isoforms. RPKM of gene body from RNA-seq was clustered into 6 clusters using the PAM clustering algorithm in R (R core team (2013) R: A language and environment for statistical computing. R foundation for Statistical Computing. Vienna, Austria, http://www.R-project.org/, Bioconductor [74]) using the z-scores calculated from the log10 (RPKM) values. GO analysis was performed with DAVID (http://david.abcc.ncifcrf.gov/).

RNAPII and H3K27ac gene body occupancy quantification

The occupancy of RNAPII and H3K27ac of the ChIP-seq datasets from HKC1 at Refseq gene transcripts (hg19) was quantified by the detection of the sequenced reads, and the reads per kilobase per million mapped reads (RPKM) was calculated for each gene.

RNAPII ChIP-seq clustering

RNAPII ChIP-seq RefSeq genes were filtered for genes with RPKM expression level of at least 1 in at least one condition, resulting in a set of 7,223 distinct genes, and 8,741 when considering different isoforms. These genes were clustered into 9 clusters using the PAM clustering algorithm in R [74] using the z-scores calculated from the $\log_2$ (RPKM) values.

RNAPII occupancy versus RNA steady-state comparison

Rank-based comparisons of expression levels were used to compare RNAPII occupancy and RNA steady state due to the different distributions of RNAPII occupancy and RNA-seq expression levels. Genes were ranked separately according to RNAPII ChIP-seq occupancy and RNA-seq RPKM. For each gene, the difference between the RNA-seq and ChIP-seq ranks was taken, and the genes were ranked according to this difference. Subsequently, the enrichment of non-coding RNAs with high RNAPII occupancy relative to RNA-seq levels was determined using mean-rank gene set enrichment analysis [75] as implemented in the "limma" R package. Overall correlations between the RNA-seq and RNAPII levels of different samples were calculated using the Spearman rank correlation coefficient, due to the fact that the genomewide gene expression profiles per sample do not follow a normal distribution.

Correlation between enhancer H3K27ac, p63 signal, and gene body RNAPII ChIP-seq signal

For all expressed genes mapped to nearby enhancers, the Pearson correlation coefficient was calculated between the H3K27ac and p63 ChIP-seq read counts at the associated enhancers (normalized for per-sample total read count) and the gene body RNAPII RPKM score across the four differentiation stages. H3K27ac enhancer signal was defined as a 4-kb window around the identified p63 ChIP-seq peak center to accommodate its broader binding pattern. When multiple enhancers mapped to a single gene, their read counts were summed.

Clustered enhancers calling

Clustered epidermal enhancers were called using the ROSE tool, version 0.1 [42]. The identified H3K27ac peaks were used to call the cl-epidermal enhancers using the same settings as described in Hnisz et al, [42], with an enhancer stitching distance of 12-kb and a 4-kb exclusion window around promoters. H3K27ac (cl-epidermal) enhancer differentiation profiles were clustered into 6 clusters using PAM clustering, applied to the z-scores of the normalized read counts.

p63-bound enriched regions were determined using the same approach and settings as the detection of cl-epidermal enhancers, except that the identified p63 peaks from p63 ChIP-seq files were used. Additionally, the 4-kb exclusion window around promoters was not used. Enriched regions consisting of only one single p63 peak were removed from the set.

Association between H3K27ac signal dynamics at single enhancers and gene body RNAPII dynamics

The H3K27ac signal at co-localized single p63 binding sites was defined by the calculation of RPKM using a 4-kb window around the identified p63 ChIP-seq peak center from the H3K27ac ChIP-seq datasets of all four differentiation stages of HKC1. To analyze H3K27ac dynamics, z-scores of $\log_2$ (RPKM) were determined and clustered into 7 clusters by K-means clustering. These enhancers were mapped to the closest gene (human genome NCBI build 37, hg19). The detected RNAPII gene body occupancy (RPKM > 1) and clustering were defined as previously described from the RNAPII ChIP-seq datasets of all four differentiation stages of HKC1. Over- and underrepresentation of shared genes associated with p63 binding sites with H3K27ac occupancy dynamics (for all 7 clusters) were compared with the gene clusters defined by RNAPII occupancy dynamics (for all 9 clusters). Significant fold enrichment or depletion was defined using hypergeometric distribution analysis

 © 2015 The Authors

(P-value < 0.001) combined with a fold change higher than 1.5 or smaller than 0.5, respectively.

Association between H3K27ac signal dynamics at cl-epidermal enhancers and gene body RNAPII dynamics

The H3K27ac signal at cl-epidermal enhancers was defined by summing the reads falling within each cl-epidermal enhancer region from the count-normalized H3K27ac ChIP-seq datasets of all four differentiation stages of HKC1. The BAM files containing the H3K27ac ChIP-seq reads were normalized to the same number of reads per dataset by randomly removing excess reads from the larger BAM files. To analyze H3K27ac dynamics, the z-scores of the normalized counts across the four differentiation stages were calculated and clustered into 6 clusters using K-means clustering. These cl-epidermal enhancers were mapped to the closest gene or any overlapping genes (human genome NCBI build 37, hg19). The detected RNAPII gene body occupancy (RPKM > 1) and clustering were defined as previously described from the RNAPII ChIP-seq datasets of all four differentiation stages of HKC1. Over- and under-representation of shared genes associated with cl-epidermal enhancer H3K27ac occupancy dynamics (for all 6 clusters) were compared with the gene clusters defined by RNAPII occupancy dynamics (for all 9 clusters). Significant fold enrichment or depletion was defined using hypergeometric distribution analysis (P-value < 0.001) combined with a fold change higher than 1.5 or smaller than 0.5, respectively.

Enrichment of p63 binding sites in clustered epidermal enhancers

Enrichment of p63 binding sites in clustered epidermal enhancers was determined by randomly shuffling the clustered enhancers across the genome using the "bedtools shuffle" command from the BEDTools suite [76], excluding unsequenced genomic gaps larger than 10 kb. Overlap with p63 binding sites was determined using the "bedtools intersect" command. The P-value of p63 binding site enrichment in clustered enhancers was determined by fitting a normal distribution to the overlap percentages for the shuffled regions (which were normally distributed, Shapiro–Wilks P-value = 0.52) and determining the area under the cumulative probability curve to the right of the actual overlap percentage.

Detected transcribed miRNAs by RNAPII occupancy

The occupancy of RNAPII ChIP-seq datasets at the transcribed miRNAs was quantified by RPKM calculation of the detected sequenced reads for each identified RNAPII peak. A cutoff of RPKM > 1 was set, and only miRNAs, smaller than 200 bp, intersecting these RNAPII peak regions were considered.

Motif enrichment analysis

Motif enrichment was determined using Gimme scan of the GimmeMotifs package [77], which was used to scan the p63BS datasets for motif enrichment with a motif score of at least 99% of known family motifs [16], including the RUNX family motifs. The p63BS datasets were centered on the peak summit of the identified p63 peaks (Supplementary Table S5) and extended 300 bp to both directions. A background file of 10,000 genomically matched random peaks was generated using Gimme background, of which a validation set (sequences not used for motif prediction) was generated using Gimme threshold of all known family motifs with a false discovery rate P-value of 0.01 (considering a motif score of at least 99%). Motif enrichment in active versus inactive p63 binding site and motif enrichment for the different p63 binding site clusters with H3K27ac occupancy was determined. For each set of p63BS sequences, a background set was generated, and the validation set was used as a cutoff file to determine enrichment in the family motifs of all p63BS datasets. We used 1.5-fold as a cutoff to determine enrichment of motifs present in the datasets versus matched genomic background datasets, and between the different datasets.

ENCODE data

H3K27ac ChIP-seq (GSM733674), H3K4me1 ChIP-seq (GSM733698), H3K27me3 ChIP-seq (GSM733701), H3K9me1 ChIP-seq (GSM733655), H3K9me3 ChIP-seq (GSM1003528), and Open chromatin by DNaseI HS (GSM816635) data from NHEK was downloaded from the ENCODE UCSC browser (http://genome.ucsc.edu/ENCODE/).

Accession codes

All RNA-seq and ChIP-seq data have been deposited in the Gene Expression Omnibus [78] (GEO GSE59827).

Supplementary information for this article is available online: http://embor.embopress.org

Acknowledgements
This work is supported by NWO/ALW/MEERVOUD/836.12.010 (HZ), NGI/BioRange program of the NBIC (MO), Radboud University fellowship (HZ), and NCMLS PhD fellowship (ENK). We thank K. Mulder for critical review of the manuscript and E. van den Bogaard for providing the keratinocyte lines. We also thank E. Janssen-Megens, K. Berentsen, and K. J. Françoijs for operating the Illumina Hi-Seq analyzer and initial data output. We thank the ENCODE Consortium, the BROAD Institute of MIT and Harvard, and Duke University for sharing their data.

Author contributions
ENK, MO, HvB, and HZ conceived and designed the experiments and analysis and wrote the manuscript. ENK, MO, HN, and HZ performed the experiments and analysis. MO, SJvH, JS, and HGS contributed reagents/materials/analysis tools.

Conflict of interest
The authors declare that they have no conflict of interest.

References

1. Rinne T, Hamel B, van Bokhoven H, Brunner HG (2006) Pattern of p63 mutations and their phenotypes–update. *Am J Med Genet A* 140: 1396 – 1406

© 2015 The Authors

2. Yang A, Schweitzer R, Sun D, Kaghad M, Walker N, Bronson RT, Tabin C, Sharpe A, Caput D, Crum C *et al* (1999) p63 is essential for regenerative proliferation in limb, craniofacial and epithelial development. *Nature* 398: 714 – 718
3. Mills AA, Zheng B, Wang XJ, Vogel H, Roop DR, Bradley A (1999) p63 is a p53 homologue required for limb and epidermal morphogenesis. *Nature* 398: 708 – 713
4. Ferone G, Thomason HA, Antonini D, De Rosa L, Hu B, Gemei M, Zhou H, Ambrosio R, Rice DP, Acampora D *et al* (2012) Mutant p63 causes defective expansion of ectodermal progenitor cells and impaired FGF signalling in AEC syndrome. *EMBO Mol Med* 4: 192 – 205
5. Lo Iacono N, Mantero S, Chiarelli A, Garcia E, Mills AA, Morasso MI, Costanzo A, Levi G, Guerrini L, Merlo GR (2008) Regulation of Dlx5 and Dlx6 gene expression by p63 is involved in EEC and SHFM congenital limb defects. *Development* 135: 1377 – 1388
6. Vernersson Lindahl E, Garcia EL, Mills AA (2013) An allelic series of Trp63 mutations defines TAp63 as a modifier of EEC syndrome. *Am J Med Genet A* 161A: 1961 – 1971
7. Medawar A, Virolle T, Rostagno P, de la Forest-Divonne S, Gambaro K, Rouleau M, Aberdam D (2008) DeltaNp63 is essential for epidermal commitment of embryonic stem cells. *PLoS ONE* 3: e3441
8. Rostagno P, Wolchinsky Z, Vigano AM, Shivtiel S, Zhou H, Van Bokhoven H, Ferone G, Missero C, Mantovani R, Aberdam D *et al* (2010) Embryonic stem cells as an ectodermal cellular model of human p63-related dysplasia syndromes. *Biochem Biophys Res Commun* 395: 131 – 135
9. Blanpain C, Fuchs E (2009) Epidermal homeostasis: a balancing act of stem cells in the skin. *Nat Rev Mol Cell Biol* 10: 207 – 217
10. Lopez-Pajares V, Yan K, Zarnegar BJ, Jameson KL, Khavari PA (2013) Genetic pathways in disorders of epidermal differentiation. *Trends Genet* 29: 31 – 40
11. Muller FB, Kuster W, Wodecki K, Almeida H Jr, Bruckner-Tuderman L, Krieg T, Korge BP, Arin MJ (2006) Novel and recurrent mutations in keratin KRT5 and KRT14 genes in epidermolysis bullosa simplex: implications for disease phenotype and keratin filament assembly. *Hum Mutat* 27: 719 – 720
12. Maestrini E, Monaco AP, McGrath JA, Ishida-Yamamoto A, Camisa C, Hovnanian A, Weeks DE, Lathrop M, Uitto J, Christiano AM (1996) A molecular defect in loricrin, the major component of the cornified cell envelope, underlies Vohwinkel's syndrome. *Nat Genet* 13: 70 – 77
13. Mulder KW, Wang X, Escriu C, Ito Y, Schwarz RF, Gillis J, Sirokmany G, Donati G, Uribe-Lewis S, Pavlidis P *et al* (2012) Diverse epigenetic strategies interact to control epidermal differentiation. *Nat Cell Biol* 14: 753 – 763
14. Truong AB, Kretz M, Ridky TW, Kimmel R, Khavari PA (2006) p63 regulates proliferation and differentiation of developmentally mature keratinocytes. *Genes Dev* 20: 3185 – 3197
15. Koster MI, Kim S, Mills AA, DeMayo FJ, Roop DR (2004) p63 is the molecular switch for initiation of an epithelial stratification program. *Genes Dev* 18: 126 – 131
16. Shen J, van den Bogaard EH, Kouwenhoven EN, Bykov VJ, Rinne T, Zhang Q, Tjabringa GS, Gilissen C, van Heeringen SJ, Schalkwijk J *et al* (2013) APR-246/PRIMA-1(MET) rescues epidermal differentiation in skin keratinocytes derived from EEC syndrome patients with p63 mutations. *Proc Natl Acad Sci USA* 110: 2157 – 2162
17. Della Gatta G, Bansal M, Ambesi-Impiombato A, Antonini D, Missero C, di Bernardo D (2008) Direct targets of the TRP63 transcription factor revealed by a combination of gene expression profiling and reverse engineering. *Genome Res* 18: 939 – 948
18. Kouwenhoven EN, van Heeringen SJ, Tena JJ, Oti M, Dutilh BE, Alonso ME, de la Calle-Mustienes E, Smeenk L, Rinne T, Parsaulian L *et al* (2010) Genome-wide profiling of p63 DNA-binding sites identifies an element that regulates gene expression during limb development in the 7q21 SHFM1 locus. *PLoS Genet* 6: e1001065
19. McDade SS, Henry AE, Pivato GP, Kozarewa I, Mitsopoulos C, Fenwick K, Assiotis I, Hakas J, Zvelebil M, Orr N *et al* (2012) Genome-wide analysis of p63 binding sites identifies AP-2 factors as co-regulators of epidermal differentiation. *Nucleic Acids Res* 40: 7190 – 7206
20. Van Ruissen F, de Jongh GJ, Zeeuwen PL, Van Erp PE, Madsen P, Schalkwijk J (1996) Induction of normal and psoriatic phenotypes in submerged keratinocyte cultures. *J Cell Physiol* 168: 442 – 452
21. Fuchs E (2008) Skin stem cells: rising to the surface. *J Cell Biol* 180: 273 – 284
22. Kretz M, Siprashvili Z, Chu C, Webster DE, Zehnder A, Qu K, Lee CS, Flockhart RJ, Groff AF, Chow J *et al* (2013) Control of somatic tissue differentiation by the long non-coding RNA TINCR. *Nature* 493: 231 – 235
23. Parsa R, Yang A, McKeon F, Green H (1999) Association of p63 with proliferative potential in normal and neoplastic human keratinocytes. *J Invest Dermatol* 113: 1099 – 1105
24. Dennis G Jr, Sherman BT, Hosack DA, Yang J, Gao W, Lane HC, Lempicki RA (2003) DAVID: Database for Annotation, Visualization, and Integrated Discovery. *Genome Biol* 4: P3
25. Kohler S, Doelken SC, Mungall CJ, Bauer S, Firth HV, Bailleul-Forestier I, Black GC, Brown DL, Brudno M, Campbell J *et al* (2014) The Human Phenotype Ontology project: linking molecular biology and disease through phenotype data. *Nucleic Acids Res* 42: D966 – D974
26. Aberdam D, Candi E, Knight RA, Melino G (2008) miRNAs, 'stemness' and skin. *Trends Biochem Sci* 33: 583 – 591
27. Candi E, Amelio I, Agostini M, Melino G (2014) MicroRNAs and p63 in epithelial stemness. *Cell Death Differ* 22: 12 – 21
28. Shenoy A, Blelloch RH (2014) Regulation of microRNA function in somatic stem cell proliferation and differentiation. *Nat Rev Mol Cell Biol* 15: 565 – 576
29. Lee Y, Kim M, Han J, Yeom KH, Lee S, Baek SH, Kim VN (2004) MicroRNA genes are transcribed by RNA polymerase II. *EMBO J* 23: 4051 – 4060
30. Lena AM, Shalom-Feuerstein R, Rivetti di Val Cervo P, Aberdam D, Knight RA, Melino G, Candi E (2008) miR-203 represses 'stemness' by repressing DeltaNp63. *Cell Death Differ* 15: 1187 – 1195
31. Yi R, Poy MN, Stoffel M, Fuchs E (2008) A skin microRNA promotes differentiation by repressing 'stemness'. *Nature* 452: 225 – 229
32. Encode Project Consortium, Bernstein BE, Birney E, Dunham I, Green ED, Gunter C, Snyder M (2012) An integrated encyclopedia of DNA elements in the human genome. *Nature* 489: 57 – 74
33. Zhu J, Adli M, Zou JY, Verstappen G, Coyne M, Zhang X, Durham T, Miri M, Deshpande V, De Jager PL *et al* (2013) Genome-wide chromatin state transitions associated with developmental and environmental cues. *Cell* 152: 642 – 654
34. Karlic R, Chung HR, Lasserre J, Vlahovicek K, Vingron M (2010) Histone modification levels are predictive for gene expression. *Proc Natl Acad Sci USA* 107: 2926 – 2931
35. van Heeringen SJ (2013) Vertebrate Motif Clusters. figshare: http://dx.doi.org/10.6084/m9.figshare.819997
36. Feuerborn A, Srivastava PK, Kuffer S, Grandy WA, Sijmonsma TP, Gretz N, Brors B, Grone HJ (2011) The Forkhead factor FoxQ1 influences epithelial differentiation. *J Cell Physiol* 226: 710 – 719
37. Wong CF, Barnes LM, Dahler AL, Smith L, Serewko-Auret MM, Popa C, Abdul-Jabbar I, Saunders NA (2003) E2F modulates keratinocyte

 © 2015 The Authors

squamous differentiation: implications for E2F inhibition in squamous cell carcinoma. *J Biol Chem* 278: 28516 – 28522

38. Ogata A, Shimizu T, Abe R, Shimizu H, Sakai M (2004) Expression of c-maf and mafB genes in the skin during rat embryonic development. *Acta Histochem* 106: 65 – 67
39. Bollag WB (2007) Differentiation of human keratinocytes requires the vitamin d receptor and its coactivators. *J Invest Dermatol* 127: 748 – 750
40. Kommagani R, Leonard MK, Lewis S, Romano RA, Sinha S, Kadakia MP (2009) Regulation of VDR by deltaNp63alpha is associated with inhibition of cell invasion. *J Cell Sci* 122: 2828 – 2835
41. Whyte WA, Orlando DA, Hnisz D, Abraham BJ, Lin CY, Kagey MH, Rahl PB, Lee TI, Young RA (2013) Master transcription factors and mediator establish super-enhancers at key cell identity genes. *Cell* 153: 307 – 319
42. Hnisz D, Abraham BJ, Lee TI, Lau A, Saint-Andre V, Sigova AA, Hoke HA, Young RA (2013) Super-enhancers in the control of cell identity and disease. *Cell* 155: 934 – 947
43. Pasquali L, Gaulton KJ, Rodriguez-Segui SA, Mularoni L, Miguel-Escalada I, Akerman I, Tena JJ, Moran I, Gomez-Marin C, van de Bunt M *et al* (2014) Pancreatic islet enhancer clusters enriched in type 2 diabetes risk-associated variants. *Nat Genet* 46: 136 – 143
44. Shimomura Y, Wajid M, Shapiro L, Christiano AM (2008) P-cadherin is a p63 target gene with a crucial role in the developing human limb bud and hair follicle. *Development* 135: 743 – 753
45. Ferone G, Mollo MR, Thomason HA, Antonini D, Zhou H, Ambrosio R, De Rosa L, Salvatore D, Getsios S, van Bokhoven H *et al* (2013) p63 control of desmosome gene expression and adhesion is compromised in AEC syndrome. *Hum Mol Genet* 22: 531 – 543
46. Sandilands A, Sutherland C, Irvine AD, McLean WH (2009) Filaggrin in the frontline: role in skin barrier function and disease. *J Cell Sci* 122: 1285 – 1294
47. Masse I, Barbollat-Boutrand L, Molina M, Berthier-Vergnes O, Joly-Tonetti N, Martin MT, Caron de Fromentel C, Kanitakis J, Lamartine J (2012) Functional interplay between p63 and p53 controls RUNX1 function in the transition from proliferation to differentiation in human keratinocytes. *Cell Death Dis* 3: e318
48. Kommagani R, Caserta TM, Kadakia MP (2006) Identification of vitamin D receptor as a target of p63. *Oncogene* 25: 3745 – 3751
49. Martynova E, Pozzi S, Basile V, Dolfini D, Zambelli F, Imbriano C, Pavesi G, Mantovani R (2012) Gain-of-function p53 mutants have widespread genomic locations partially overlapping with p63. *Oncotarget* 3: 132 – 143
50. Tran MN, Choi W, Wszolek MF, Navai N, Lee IL, Nitti G, Wen S, Flores ER, Siefker-Radtke A, Czerniak B *et al* (2013) The p63 protein isoform DeltaNp63alpha inhibits epithelial-mesenchymal transition in human bladder cancer cells: role of MIR-205. *J Biol Chem* 288: 3275 – 3288
51. Tucci P, Agostini M, Grespi F, Markert EK, Terrinoni A, Vousden KH, Muller PA, Dotsch V, Kehrloesser S, Sayan BS *et al* (2012) Loss of p63 and its microRNA-205 target results in enhanced cell migration and metastasis in prostate cancer. *Proc Natl Acad Sci USA* 109: 15312 – 15317
52. van den Bogaard EH, Bergboer JG, Vonk-Bergers M, van Vlijmen-Willems IM, Hato SV, der van Valk PG, Schroder JM, Joosten I, Zeeuwen PL, Schalkwijk J (2013) Coal tar induces AHR-dependent skin barrier repair in atopic dermatitis. *J Clin Invest* 123: 917 – 927
53. Rizzo JM, Romano RA, Bard J, Sinha S (2014) RNA-seq studies reveal new insights into p63 and the transcriptomic landscape of the mouse skin. *J Invest Dermatol* 135: 629 – 632
54. Romano RA, Smalley K, Magraw C, Serna VA, Kurita T, Raghavan S, Sinha S (2012) DeltaNp63 knockout mice reveal its indispensable role as a master regulator of epithelial development and differentiation. *Development* 139: 772 – 782
55. Chakravarti D, Su X, Cho MS, Bui NH, Coarfa C, Venkatanarayan A, Benham AL, Flores Gonzalez RE, Alana J, Xiao W *et al* (2014) Induced multipotency in adult keratinocytes through down-regulation of DeltaNp63 or DGCR8. *Proc Natl Acad Sci USA* 111: E572 – E581
56. Bartel DP (2004) MicroRNAs: genomics, biogenesis, mechanism, and function. *Cell* 116: 281 – 297
57. Cullen BR (2004) Transcription and processing of human microRNA precursors. *Mol Cell* 16: 861 – 865
58. Sudou N, Yamamoto S, Ogino H, Taira M (2012) Dynamic in vivo binding of transcription factors to cis-regulatory modules of cer and gsc in the stepwise formation of the Spemann-Mangold organizer. *Development* 139: 1651 – 1661
59. Rada-Iglesias A, Bajpai R, Prescott S, Brugmann SA, Swigut T, Wysocka J (2012) Epigenomic annotation of enhancers predicts transcriptional regulators of human neural crest. *Cell Stem Cell* 11: 633 – 648
60. Thomason HA, Zhou H, Kouwenhoven EN, Dotto GP, Restivo G, Nguyen BC, Little H, Dixon MJ, van Bokhoven H, Dixon J (2010) Cooperation between the transcription factors p63 and IRF6 is essential to prevent cleft palate in mice. *J Clin Invest* 120: 1561 – 1569
61. Fakhouri WD, Rahimov F, Attanasio C, Kouwenhoven EN, Ferreira De Lima RL, Felix TM, Nitschke L, Huver D, Barrons J, Kousa YA *et al* (2014) An etiologic regulatory mutation in IRF6 with loss- and gain-of-function effects. *Hum Mol Genet* 23: 2711 – 2720
62. Zaret KS, Carroll JS (2011) Pioneer transcription factors: establishing competence for gene expression. *Genes Dev* 25: 2227 – 2241
63. Rheinwald JG, Green H (1977) Epidermal growth factor and the multiplication of cultured human epidermal keratinocytes. *Nature* 265: 421 – 424
64. Rinne T, Clements SE, Lamme E, Duijf PH, Bolat E, Meijer R, Scheffer H, Rosser E, Tan TY, McGrath JA *et al* (2008) A novel translation re-initiation mechanism for the p63 gene revealed by amino-terminal truncating mutations in Rapp-Hodgkin/Hay-Wells-like syndromes. *Hum Mol Genet* 17: 1968 – 1977
65. Smeenk L, van Heeringen SJ, Koeppel M, van Driel MA, Bartels SJ, Akkers RC, Denissov S, Stunnenberg HG, Lohrum M (2008) Characterization of genome-wide p53-binding sites upon stress response. *Nucleic Acids Res* 36: 3639 – 3654
66. Livak KJ, Schmittgen TD (2001) Analysis of relative gene expression data using real-time quantitative PCR and the 2(−Delta Delta C(T)) Method. *Methods* 25: 402 – 408
67. Li H, Durbin R (2010) Fast and accurate long-read alignment with Burrows–Wheeler transform. *Bioinformatics* 26: 589 – 595
68. Feng J, Liu T, Qin B, Zhang Y, Liu XS (2012) Identifying ChIP-seq enrichment using MACS. *Nat Protoc* 7: 1728 – 1740
69. Wu TD, Nacu S (2010) Fast and SNP-tolerant detection of complex variants and splicing in short reads. *Bioinformatics* 26: 873 – 881
70. Flicek P, Ahmed I, Amode MR, Barrell D, Beal K, Brent S, Carvalho-Silva D, Clapham P, Coates G, Fairley S *et al* (2013) Ensembl 2013. *Nucleic Acids Res* 41: D48 – D55
71. Trapnell C, Williams BA, Pertea G, Mortazavi A, Kwan G, van Baren MJ, Salzberg SL, Wold BJ, Pachter L (2010) Transcript assembly and quantification by RNA-Seq reveals unannotated transcripts and isoform switching during cell differentiation. *Nat Biotechnol* 28: 511 – 515
72. Pruitt KD, Brown GR, Hiatt SM, Thibaud-Nissen F, Astashyn A, Ermolaeva O, Farrell CM, Hart J, Landrum MJ, McGarvey KM *et al* (2014) RefSeq: an update on mammalian reference sequences. *Nucleic Acids Res* 42: D756 – D763

© 2015 The Authors

73. Meyer LR, Zweig AS, Hinrichs AS, Karolchik D, Kuhn RM, Wong M, Sloan CA, Rosenbloom KR, Roe G, Rhead B *et al* (2013) The UCSC Genome Browser database: extensions and updates 2013. *Nucleic Acids Res* 41: D64 – D69
74. Gentleman RC, Carey VJ, Bates DM, Bolstad B, Dettling M, Dudoit S, Ellis B, Gautier L, Ge Y, Gentry J *et al* (2004) Bioconductor: open software development for computational biology and bioinformatics. *Genome Biol* 5: R80
75. Michaud J, Simpson KM, Escher R, Buchet-Poyau K, Beissbarth T, Carmichael C, Ritchie ME, Schutz F, Cannon P, Liu M *et al* (2008) Integrative analysis of RUNX1 downstream pathways and target genes. *BMC Genom* 9: 363
76. Quinlan AR, Hall IM (2010) BEDTools: a flexible suite of utilities for comparing genomic features. *Bioinformatics* 26: 841 – 842
77. van Heeringen SJ, Veenstra GJ (2011) GimmeMotifs: a de novo motif prediction pipeline for ChIP-sequencing experiments. *Bioinformatics* 27: 270 – 271
78. Edgar R, Domrachev M, Lash AE (2002) Gene Expression Omnibus: NCBI gene expression and hybridization array data repository. *Nucleic Acids Res* 30: 207 – 210

License: This is an open access article under the terms of the Creative Commons Attribution-NonCommercial-NoDerivs 4.0 License, which permits use and distribution in any medium, provided the original work is properly cited, the use is non-commercial and no modifications or adaptations are made.

 © 2015 The Authors